Plant Soil
https://doi.org/10.1007/s11104-018-3805-4

REGULAR ARTICLE

A half-type ABC transporter FeSTAR1 regulates Al resistance possibly via UDP-glucose-based hemicellulose metabolism and Al binding

Jia Meng Xu · He Qiang Lou · Jian Feng Jin · Wei Wei Chen · Jiang Xue Wan · Wei Fan · Jian Li Yang

Received: 11 July 2018 / Accepted: 28 August 2018

Abstract
Aims Buckwheat (*Fagopyrum esculentum*) is highly tolerant to Al stress, but the molecular mechanisms remain largely unknown. This study aims to investigate a half-type ABC transporter gene (*FeSTAR1*) with respect to Al tolerance.
Methods The expression of *FeSTAR1* was examined and complementation test in *atstar1* mutant was conducted. Furthermore, Al distribution and cell wall polysaccharides content were analyzed.
Results FeSTAR1 is an ABC transporter protein with nucleotide binding domain, but lack of transmembrane domain. Consistently, FeSTAR1 is a soluble protein, localizing to both cytoplasm and nucleus. Al rapidly and specifically induced *FeSTAR1* expression. Heterologous expression of FeSTAR1 in *atstar1* rescued its Al tolerance, and exogenous applied UDP-glucose could alleviate Al sensitivity of *atstar1* mutant, suggesting the connection between FeSTAR1 and UDP-glucose in terms of Al tolerance. Furthermore, FeSTAR1 complemented lines accumulated less Al in root cell wall than *atstar1* mutant. Further cell wall fraction analysis showed that Al was largely confined to cell wall hemicellulose1, at which Al content was significantly lower in complemented lines. Consistent with Al distribution in different cell wall polysaccharides, complemented lines had lower hemicellulose1 content.
Conclusion Our results indicate that FeSTAR1 is involved in Al resistance via possibly cell wall matrix polysaccharides metabolism in buckwheat.

Keywords Aluminum toxicity · Cell wall · Matrix polysaccharides · UDP-glucose

Responsible Editor: Juan Barcelo.

Electronic supplementary material The online version of this article (https://doi.org/10.1007/s11104-018-3805-4) contains supplementary material, which is available to authorized users.

J. M. Xu · J. F. Jin · J. X. Wan · J. L. Yang (✉)
State Key Laboratory of Plant Physiology and Biochemistry, College of Life Sciences, Zhejiang University, Hangzhou, China
e-mail: yangjianli@zju.edu.cn

H. Q. Lou
State Key Laboratory of Subtropical Silviculture, School of Forestry and Biotechnology, Zhejiang A& F University, Lin'an, Zhejiang 311300, China

W. W. Chen
College of Life and Environmental Sciences, Hangzhou Normal University, Hangzhou 310036, China

W. Fan
State Key Laboratory of Conservation and Utilization of Bio-resources in Yunnan, The Key Laboratory of Medicinal Plant Biology of Yunnan Province, National & Local Joint Engineering Research Center on Germplasm Innovation & Utilization of Chinese Medicinal Materials in Southwest China, Yunnan Agricultural University, Kunming 650201, China

Introduction

Approximately 30% of the earth's total land area consists of acid soils, and as much as 50% of the world's potential arable land are acidic (Bojórquez-Quintal et al.

Published online: 05 September 2018

2017; Von Uexküll and Mutert 1995). Aluminum (Al) is the most abundant metal element in the earth's crust and usually exists as nonphytotoxic and insoluble complex with silicon and oxygen. However, at the soil pH ≤ 5.0, Al gets solubilized and present in the form of Al^{3+} as the most toxic Al species in the soil solution. Al^{3+} at micromolar concentrations could inhibit root elongation in a short period of time, which in turn limits water and mineral nutrient uptake, ultimately resulting in reduced crop yields (Delhaize and Ryan 1995).

There exist considerable difference in aluminum resistance among different plant species and genotypes (Yang et al. 2005). As an Al-accumulating crop, common buckwheat (*Fagopyrum esculentum* Moench.) has evolved from long-term adaptation to aluminum toxicity a series of Al resistant mechanisms different from the model plants Arabidopsis thaliana and rice. Fox example, oxalic acid can be rapidly released into rhizosphere from buckwheat root tip to detoxify Al externally (Klug and Horst 2010; Zheng et al. 1998, 2005). Once Al is taken up by the root, it is chelated with oxalate to form a 1:3 Al-oxalate complex and then segregated into vacuoles (Ma et al. 1998). Also, Al can be translocated from the roots to the shoots in the form of Al-citrate complex, suggesting that ligand exchange occurs during xylem loading (Ma and Hiradate 2000). After xylem unloading, Al can be complexed by oxalate or citrate depending upon Al concentrations and compartmentalized into leaf vacuoles (Shen et al. 2002, 2004).

Although great progresses have been made toward unveiling the physiological mechanisms of buckwheat aluminum stress responses, the molecular mechanisms remain largely unknown. Recently, transcriptomic analyses were carried out to dissect global changes of gene expression in response to Al stress (Yokosho et al. 2014; Zhu et al. 2015). Furthermore, genome assembly in tartary buckwheat (*Fagopyrum tataricum*) greatly facilitates the identification and characterization of genes involved in Al resistance (Zhang et al. 2017). We performed transcriptomic analysis of the apex and the leaves of buckwheat treated with 20 μM Al for 6 h and found that only five transporter genes, *FeMATE1* (*multidrug and toxic compound extrusion 1*), *FeALS1*, (*ALUMINUM SENSITIVE1*), *FeSTAR1* (Sensitive to Al rhizotoxicity1), *FeSTAR2*, and a divalent ion transporter gene, were up-regulated by Al in both roots and leaves (Chen et al. 2017; Xu et al. 2017). In buckwheat variety Mancan, a cDNA fragment homologous to an ABC transporter-like gene *FeALS3* [also known as *FeSTAR2* (Yokosho et al. 2014; Zhu et al. 2015; Xu et al. 2017)] has been reported to be involved in Al resistance, but its biological functions has to be investigated (Reyna-Llorens et al. 2015). FeMATE1 localizes on the plasma membrane and is responsible for secreting citric acid into the rhizosphere for external detoxification (Lei et al. 2017b). The two half-size ABC transporters, FeALS1.1 and FeALS1.2 were localized to the tonoplast responsible for compartmenting Al into the vacuoles and thus involved in internal detoxification mechanism in the roots and the leaves of buckwheat (Lei et al. 2017a). However, FeSTAR1 as well as others has not been functionally characterized yet.

Rice (*Oryza sativa*) OsSTAR1 and Arabidopsis (*Arabidopsis thaliana*) AtSTAR1 have been reported to play important role in Al resistance (Huang et al. 2009; Huang et al. 2010). OsSTAR1 interacts with OsSTAR2 to transport UDP-Glc to the apoplast presumably for modifying the Al-sensitive part of the cell wall, and thus gets involved in Al resistance in rice (Huang et al. 2009). However, it is unclear which component of the cell wall is the target of modification and whether AtSTAR1 functions similar to OsSTAR1. In the present study, we investigated the expression pattern, subcellular localization, and function of FeSTAR1. We investigated the function of FeSTAR1 by a complementation test in the Arabidopsis atstar1 mutant. Our results showed that FeSTAR1 was mainly localized to cytoplasm and nucleus, and could complement atstar1 mutant Al-sensitive phenotype. We further demonstrate that STAR1 protein involves in Al resistance by affecting cell wall hemicellulose1 metabolism.

Materials and methods

Plant materials

A previous reported Al-tolerant buckwheat cultivar Jiangxi (*Fagopyrum esculentum* Moench) was used in this study (Zheng et al. 2005). For construction of Arabidopsis transgenic lines, the coding sequence of *FeSTAR1* with or without the stop codon was cloned in-frame in front of the GFP coding region in the modified pCAMBIA1300 vector using gene-specific primers (Table S1), thus placing *FeSTAR1* or *FeSTAR1-GFP* under the control of the *35S* promoter. The constructed vectors were transformed into Arabidopsis wild-type (Col-0) and *atstar1* mutants by

agrobacterium-mediated transformation to obtain *FeSTAR1OE* (for gene function characterization), *FeSTAR1::GFP* (for subcellular localization) and *FeSTAR1OE::star1* transgenic lines (for complementation test).

For GUS reporter lines construction, a 1.7 Kb promoter sequence of *FeSTAR1* was obtained by genome walking using the Genome Walker Universal Kit (Clontech Laboratories). In brief, four genome walker libraries were constructed by digesting separate aliquots of DNA with four different restriction enzymes (*DraI*, *EcoRV*, *PvuII*, and *StuI*), followed by ligation to a genome walker adaptor. The outer/inner adaptor primers provided by the kit and a series of *FeSTAR1* gene-specific primers (Table S1) were used to perform the nested PCR. Sequences extending upstream of the cDNA sequence were isolated as the 5′-upstream regions of the gene. 1.7 Kb 5′-upstream regions of *FeSTAR1* was amplified from genome of buckwheat, then cloned to pCAMBIA1301 vector as a fusion to the β-glucuronidase (GUS) gene and finally transformed into Arabidopsis wild-type (Col-0) plants by agrobacterium-mediated transformation to obtain *FeSTAR1pro::GUS* transgenic lines.

Culture and treatments

Seeds of buckwheat were washed with deionized water thoroughly and soaked in deionized water overnight after sterilized with 5% (*v*/v) NaClO for 10 min. Then, seeds were wrapped with two-layer gauze for germination in the dark at 26 °C. Germinated seeds were transferred to a net tray floating on a 5 L of 0.5 mM $CaCl_2$ solution (pH 4.5). The solution was renewed daily. For dose-response experiment, 3-day-old seedlings were subjected to 0.5 mM $CaCl_2$ solution (pH 4.5) containing 0, 10, 20, 40, or 60 μM $AlCl_3$ for 24 h. For time-course experiment, 3-day-old seedlings were subjected to 0.5 mM $CaCl_2$ solution (pH 4.5) containing 20 μM $AlCl_3$ for 0, 3, 6, 12, or 24 h. To exam gene expression sepecificity, 3-day-old seedlings were subjected to 0.5 mM $CaCl_2$ solution (pH 4.5) containing 20 μM Al, 1 μM Cu, 20 μM Cd or 20 μM La for 24 h. The experiments were conducted in an environmentally controlled growth room with photoperiod of 14 h, day 26 °C and night 22 °C, and light intensity of 300 μmol photons m^{-2} s^{-1}.

Arabidopsis seeds were sterilized with 75% ethanol for 5 min, washed three times with sterile water. For Al resistance assay, the sterilized seeds were sowed on the 1/2 MS medium (Pi concentration reduced to 100 μM, pH 4.5 to reduce the interaction between Pi and Al^{3+}) containing 0 or 300 μM Al. Plates were kept at 4 °C for 3 d and then seeds were germinated and grown in a plant incubator with photoperiod of 16 h, day 24 °C and night 22 °C, and light intensity of 100 μmol photons m^{-2} s^{-1}.

RNA isolation and RT-PCR analysis

RNA isolation was facilitated by an RNeasy Mini Kit (Qiagen) according to the protocol. One μg of total RNA was transcribed into first-strand cDNA using TaKaRa PrimeScript™ RT Master Mix**.** The real-time quantitative RT-PCR (qRT-PCR) was carried out with SYBR® Premix Ex Taq (TAKARA) on Roche Light Cycler 480. The primer sequences were listed in Table S1. The reaction conditions were 45 cycles at 95 °C for 15 s, 56 °C for 10 s, and 72 °C for 15 s. Expression levels were normalized relative to the expression level of the *18S rRNA* (as internal control in buckwheat). All quantitative RT-PCR experiments were done three repeats from different biological samples.

The semi-quantitative RT-PCR is performed to exam expression levels of *FeSTAR1* in transgenic lines. *AtUBQ1* (as the internal control) and *FeSTAR1* cDNA were amplified using rTaq DNA polymerase with the primers listed in supplemental Table S1. PCR was carried out as follows: 94 °C for 3 min, 26 (*FeSTAR1*) or 24 cycles (*AtUBQ1*) of 94 °C denaturing for 30 s, 56 °C annealing for 1 min and 72 °C extension for 30 s, and a final 5 min extension at 72 °C.

Subcellular localization

The agrobacterium strain (GV3101) harboring 35S::FeSTAR1::GFP plasmid was transformed into Arabidopsis. The homozygous T3 transgenic seedlings were used for subcellular localization. The green fluorescence of FeSTAR1-GFP fusion proteins was observed using confocal laser scanning microscopy (LSM710; Carl Zeiss, Jena, Germany).

GUS staining

Seedlings of GUS reporter transgenic lines grown on agar medium were transferred to one-fifth Hoagland nutrition solution (pH 5.5) for 2 days and then transferred to one-fifth Hoagland nutrition solution under

low phosphate (pH 5.0, 10 μM Pi) with or without 7 μM Al. GUS staining was carried out according to Jefferson et al. (1987) with minor modifications. The staining solution (10 mL) consists of 5 mL phosphate buffer (50 mM, pH 7.0), 0.2 mL EDTA (0.5 M, pH 8.0), 0.1 mL potassium ferricyanide (50 mM), 0.1 mL potassium ferrocyanide (50 mM), 0.1 mL 10% TritonX-100, 10 mg–20 mg X-Gluc, being made up to 10 mL with ddH_2O and stored at 4 °C until use.

Root cell wall extraction and fractionation

Extraction of root crude cell wall materials and subsequent fractionation of cell wall components were performed according to Yang et al. (2008) with minor modifications. Roots were ground into fine powder in liquid nitrogen and then homogenized with 75% ethanol for 20 min in an ice-cold water bath. The sample was then centrifuged at 17,000 g for 10 min, and the supernatant was removed. The pellets were homogenized and washed with acetone, methanol:chloroform at a ratio of 1:1, and methanol, respectively. The remaining pellet (i.e., the cell wall material) was dried and stored at 4 °C for further use. Cell wall fractionation was following Yang et al. (2011). Briefly, pectin was extracted three times in boiling water for 1 h each, and supernatants were pooled. Pellets were subjected twice to a solution containing with 4% KOH and 0.1% $NaBH_4$ at room temperature for 12 h, followed by similar extraction with a solution containing 24% KOH and 0.1% $NaBH_4$. The pooled supernatants from 4 and 24% KOH extraction thus yielded the HC1 and HC2 fractions, respectively.

Determination of content of cell wall components

For quantifying pectin, uronic acid was assayed in pectin extracts according to Blumenkrantz and Asboe-Hansen (1973) using GalUA (Sigma) as a standard, thus expressed as GalUA equivalent (GaE). For HC1 and HC2 quantification, phenol sulfuric acid method (Dubois et al. 1956) was followed using glucose as a standard.

Al content measurement

For root total Al content measurement, the roots were excised after washing three times with 0.5 mM $CaCl_2$, blot dry, and digested with HNO_3. For cell sap and cell wall Al quantification, treated roots were washed with 0.5 mM $CaCl_2$, blot dry and then placed into Ultrafree-MC Centrifugal Filter Units (Millipore). After centrifuged at 3000 *g* for 10 min at 4 °C to remove solution in water free space, the roots were frozen at −80 °C overnight. The root cell sap solution was obtained by thawing the samples at room temperature and then centrifuging at 20,600 *g* for 10 min. The residual cell walls were washed with 70% (*v*/v) ethanol three times before being immersed in 0.5 mL of 2 N HCl for 36 h with occasional vortexing. The Al in the root, symplastic solution, and cell wall extracts was determined by inductively coupled plasma-atomic emission spectrometry (IRIS/AP optical emission spectrometer).

Statistical analysis

Statistical analyses were conducted by Tukey's test among treatments or one-way ANOVA test between genotypes ($p < 0.05$) with DPS 11.0 edition for windows (Tang and Zhang 2012).

Results

Isolation and sequence analysis of *FeSTAR1* in buckwheat

On the basis of buckwheat root tip transcriptomic analysis in response to Al stress (Xu et al. 2017), we obtained a full-length *FeSTAR1* cDNA via rapid amplification of cDNA ends (RACE)-PCR method (GenBank accession no. MH558683). The *FeSTAR1* coding region is 801 bp in length, and encodes a protein of 266 amino acids. Genomic sequence analysis revealed that FeSTAR1 has three introns, which is similar to OsSTAR1 but different from AtSTAR1 containing only one intron (Fig. 1a). As with OsSTAR1 and AtSTAR1, FeSTAR1 contains all the typical motifs conserved in a nucleotide binding domain (NBD) of a putative ABC transporter protein, namely, the Walker-A, Q-loop, ABC signature, Walker-B, D-loop, and H-loop motifs (Fig. 1b). FeSTAR1 shows 51.3 and 68.03% identity with OsSTAR1 and AtSTAR1, respectively (Fig. 1b). Phylogenetic relationship analysis indicated that FeSTAR1 was more closely related to Arabidopsis AtSTAR1 than rice OsSTAR1 (Supplemental Fig. S1). In most analyzed dicots and monocots, only one gene was found to encode STAR1 in their genomes, except tomato

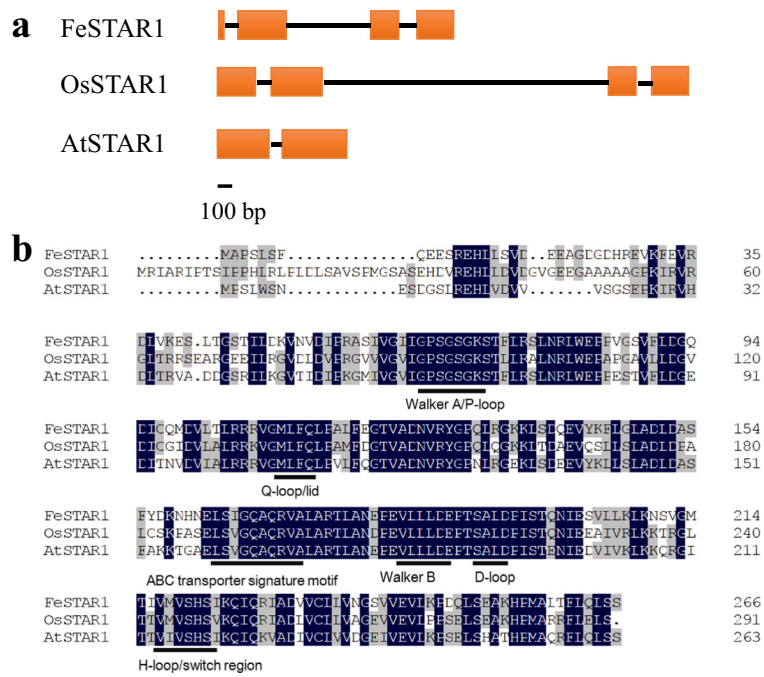

Fig. 1 Sequence analysis of *FeSTAR1*. **a** Gene structure of *STAR1* **b** Amino acid sequence alignment of STAR1 proteins from buckwheat (FeSTAR1; MH558683), rice (OsSTAR1; Os06g48060), and Arabidopsis (AtSTAR1; At1g67940)

(*Solanum lycopersicum*) and potato (*Solanum tuberosum*), both of which contains two encoding genes (Supplemental Fig. S1).

Expression pattern of FeSTAR1

RNA-seq analysis showed that the expression of *FeSTAR1* is induced by Al stress in both root tip and leaf of buckwheat (Chen et al. 2017; Xu et al. 2017). Here, we used quantitative real-time PCR (qRT-PCR) to characterize the expression of *FeSTAR1* comprehensively. Time-course experiment showed that the expression of *FeSTAR1* was dramatically induced by Al stress in the first 6 h. After 24 h, there was more than 100-fold increase, although this increase had fallen in comparison with 6 h of exposure (Fig. 2a). In a dose-response experiment, the expression of FeSTAR1 increased with increasing Al concentrations after 6 h of exposure (Fig. 2b). We next checked spatial expression of FeSTAR1 under Al stress. Consistent with our previous RNA-seq analysis, not only in roots but also in leaves the expression of FeSTAR1 was responsive to Al (Fig. 2c). To investigate the specificity of *FeSTAR1* expression, we compared its expression in response to Al with other metals. Although other metals could induce *FeSTAR1* expression slightly, the induction was significantly lower than Al stress (Fig. 2d).

To further investigate the tissue-specific localization of FeSTAR1 expression, a 1743-bp DNA sequence upstream of the translation start codon (ATG) was isolated (Supplemental Fig. S2). This promoter fragment was fused to a GUS reporter gene and transformed into Arabidopsis wild-type plants. As shown in Fig. 2e, GUS activity could be observed in the whole plants in the absence of Al stress. Compared to shoots, Al stress resulted in the increase of GUS activity more prominent in the roots. In root tip, Al stress increased GUS activity significantly. However, it seems that the induction of GUS activity in Arabidopsis root tip was weaker than the expression induction of FeSTAR1 in buckwheat root tip. This discrepancy may be due to the fact that the regulatory components differ between buckwheat and Arabidopsis. Alternatively, the promoter of FeSTAR1 may do not contain all the regulatory regions associated with induction by Al.

Subcellular location of FeSTAR1

OsSTAR1 was reported to be present at membrane fraction (Huang et al. 2009). However, STAR1 protein contains only an NBD without transmembrane domains (Fig. 1b). In order to investigate its subcellular localization, we constructed transgenic Arabidopsis plants overexpressing a FeSTAR1-GFP fusion protein under the

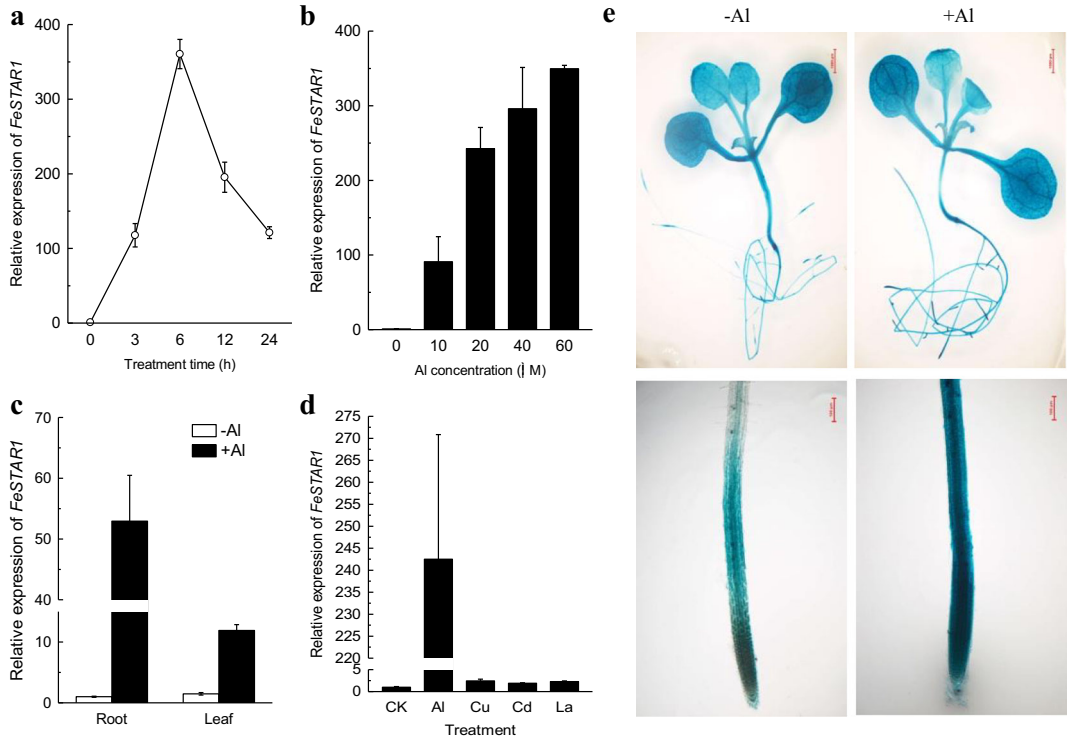

Fig. 2 Expression pattern of *FeSTAR1*. **a** time-course analysis of *FeSTAR1* expression in the root tip (0–1 cm) of buckwheat in response to 20 μM Al treatment. **b** dose-response of *FeSTAR1* expression to Al stress for 6 h in the root tip (0–1 cm) of buckwheat. **c** specificity of *FeSTAR1* expression to Al in the root tip (0–1 cm) of buckwheat. Concentrations of Al (20 μM), Cu (1 μM), Cd (20 μM) or La (20 μM) were used. Treatment was conducted for 6 h. **d** the expression level of *FeSTAR1* in the root and leaf of buckwheat under 25 μM Al treated for 6 h. Bars in (a) to (d) represent the mean ± SD of three biological replicates each with three technical replicates. (e) GUS activity staining in *FeSTAR1p::GUS* transgenic lines treated with or without Al (300 μM) for 6 h. Bar represents 1 mm (upper panel), or 200 μm (lower panel)

control of cauliflower mosaic virus 35S promoter. In mature root region where cytoplasm and organelles are crushed to cell edge by a large vacuole, GFP signal was observed in cell edge and nucleus (Fig. 3a). In the meristem of root apex, in which nuclei were present at the center of dividing cells, GFP signal was also observed both at cytoplasm and nuclei (Fig. 3b). Thus, the present result indicates that FeSTAR1 is a soluble protein without specific subcellular localization.

Complementation of *atstar1* mutants with FeSTAR1

To investigate the role of FeSTAR1 with respect to Al tolerance, Arabidopsis Al-sensitive mutant *atstar1* was used to perform complementation test. We introduced FeSTAR1 into atstar1 mutant under the control of 35S CaMV promoter. RT-PCR analysis showed that FeSTAR1 was transcriptionally expressed in two randomly selected transgenic lines (Comp.#1 and Comp.#2), whereas it was absent in both WT and atstar1 mutant plants (Fig. 4a). In the absence of Al, the root growth was similar among different genotypes (Fig. 4b). While the roots of *atstar1* were more severely inhibited than that of WT, those of the two complemented lines were similar with WT (Fig. 4b). The relative root elongation was inhibited by 60% in atstar1, but that of WT as well as two complemented lines was only inhibited by around 30% (Fig. 4c). These results suggest that FeSTAR1 is a functional homolog of AtSTAR1 in terms of Al tolerance.

Exogenous UDP-glucose recovers *atstar1* Al sensitivity

Because exogenous applied UDP-Glucose could alleviate significantly the Al-induced root growth inhibition in rice *osstar1* mutant (Huang et al. 2009), we asked whether this effect holds true in Arabidopsis *atstar1* mutant. In the absence of Al, UDP-Glc did not affect root growth of either the WT or the mutant (Fig. 5a). However, in the

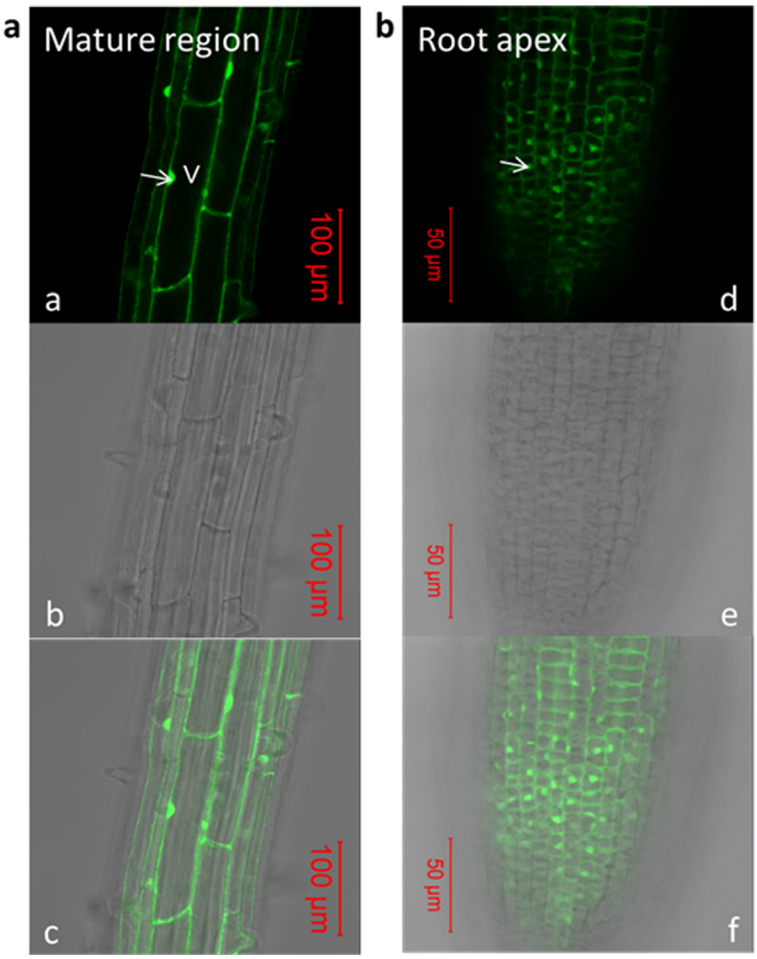

Fig. 3 Subcellular location of FeSTAR1. *35S:FeSTAR1-GFP* was stably expressed in Arabidopsis root. Arrow indicated GFP signal in cytoplasm. (**a** and **b**) GFP fluorescence. (**b** and **e**) bright field. (**c** and **f**) merged. Arrow points to nucleus. V: vacuole

presence of Al, exogenous UDP-Glucose significantly alleviated the Al-induced inhibition of root growth in the mutant (Fig. 5b). These results suggest that UDP-Glucose is involved in STAR1-mediated Al resistance.

FeSTAR1 reduces Al binding to cell wall

Al resistance could be attributed to the mechanisms of either external Al exclusion or internal Al tolerance (Kochian 1995). To further investigate the function of FeSTAR1, we analyzed Al content in apoplast and symplast. Compared with WT roots, *atstar1* mutant roots accumulated significantly more Al (Fig. 6a). However, both complemented lines showed reduced Al accumulation comparable to the levels of WT plants, suggesting that external exclusion mechanisms are related to STAR1-mediated Al tolerance. When Al concentrations in cell wall fraction and cell sap were separately analyzed, it is cell wall that accumulated moderately more Al in the *atstar1* mutant roots (Fig. 6b). There was no difference in cell sap Al concentrations among different genotypes (Fig. 6c).

Based on extractability, cell wall fundamentally comprises pectin, hemicellulose and cellulose (Keegstra 2010), and recent evidence suggest that pectin and hemicellulose contribute to Al binding (Yang et al. 2008, 2011). To further dissect which component is involved in increased Al binding to cell wall, we analyzed Al concentrations at different polysaccharides fractions. Consistent with previous report (Yang et al. 2011), cell wall hemicellulose1 fraction accumulated the majority of cell wall Al in comparison to pectin and hemicellulose2 (Fig. 7a,c). Neither pectin nor hemicellulose2 showed differential Al concentration among different genotypes. However, HC1 fraction bonded more Al in atstar1 mutant than others (Fig. 7b).

We next analyzed cell wall polysaccharides content. In *atstar1*, pectin content was lower, albeit not

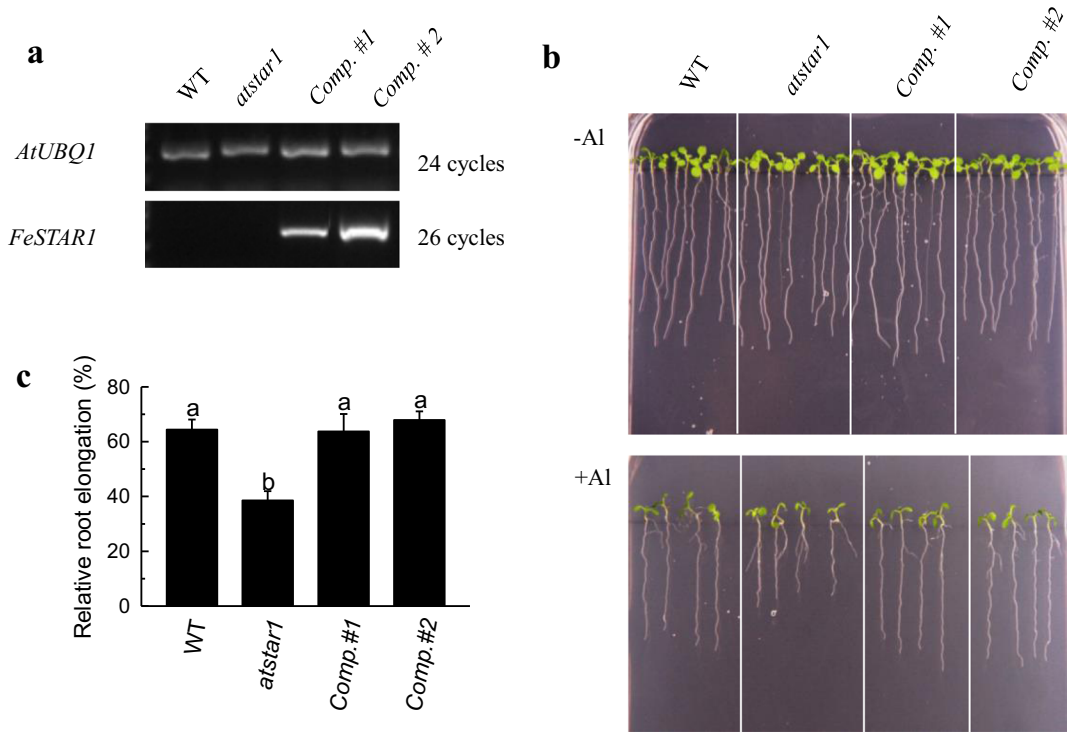

Fig. 4 ***FeSTAR1*** **rescues phenotype of** ***atstar1*** **under Al stress.** **a** *FeSTAR1* expression analysis in WT, *atstar1* and two complemented transgenic lines, i.e. Comp.#1 and Comp.#2. RT-PCR was performed to detect the mRNA levels of *FeSTAR1* (26 cycles) and the internal control *AtUBQ1* (24 cycles). **b** Phenotype of WT, *atstar1* and two complemented transgenic lines with or without Al (300 μM) stress for 7 days. **c** Relative root elongation of seedlings in response to Al for 7 days. Data are means ± SD ($n = 24$). Different letters indicate significant differences at $p < 0.05$ by Tukey'st test

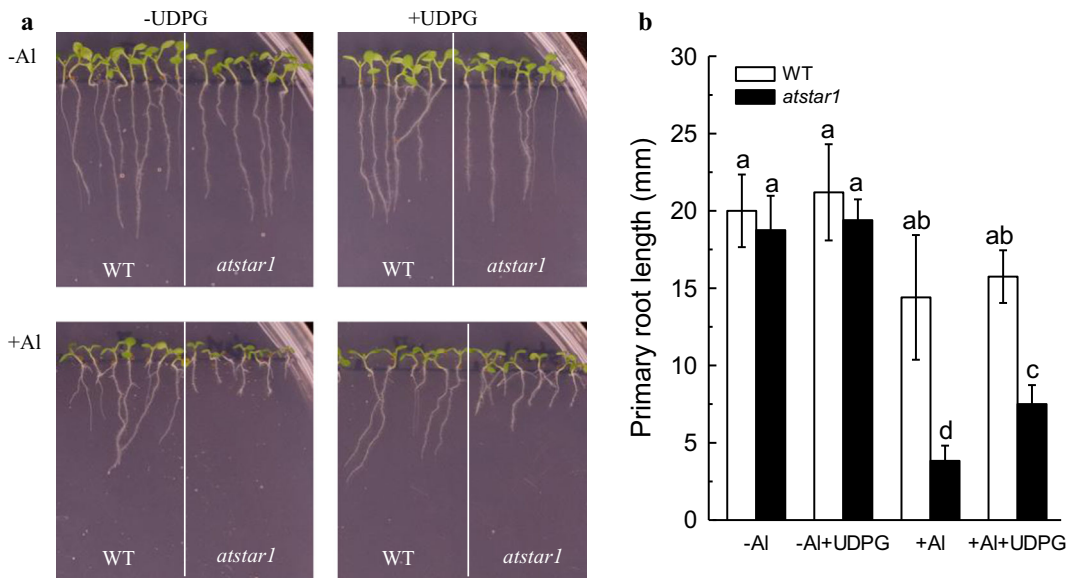

Fig. 5 Exogenous UDP-glucose partially rescued phenotype of ***atstar1*** **under Al stress. a** The effect of exogenous UDP-Glc on the phenotype of WT and *atstar1* under Al stress. **b** Primary root length of seedlings in A. Data are means ± SD ($n = 8$). Different letters indicate significant differences at $p < 0.05$ by Tukey'st test

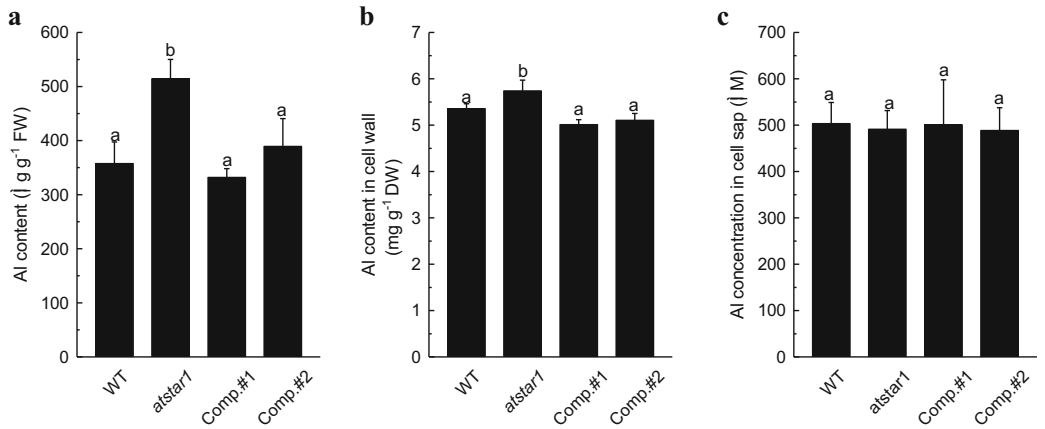

Fig. 6 Al content in the whole root (a), cell wall (b) and cell sap (c). Cell wall and cell sap was isolated from root of 4-week-old WT, atstar1 and FeSTAR1 complemented transgenic lines under 50 μM Al treatment for 24 h. Al content was determined by ICP-OES. Data are means ± SD ($n = 3$). Different letters indicate significant differences at $p < 0.05$ by Tukey'st test

significant, than WT, and complementation with FeSTAR1 recovered pectin content (Fig. 8a). By contrast, HC1 content was significantly higher in *atstar1* mutant than WT and two complemented lines especially after Al exposure (Fig. 8b). There was a little more HC2 content in *atstar1*, but it was not statistically significant (Fig. 8c). Therefore, it appears that STAR1 protein is involved in regulating the composition of cell walls which contributes to differential Al adsorption on cell wall.

Discussion

In this present study, we characterized a half-type ABC transporter FeSTAR1 with respect to Al resistance in buckwheat. The results suggested that FeSTAR1 is a functional homolog of AtSTAR1 and possibly OsSTAR1. Our conclusion is based on the following lines of evidence. First, FeSTAR1 could complement AtSTAR1 in terms of Al sensitivity (Fig. 4). Second, STAR1 proteins have consistent conserved motifs, suggesting the similar functions that they play (Fig. 1).

We further demonstrated that the FeSTAR1-mediated alleviation of Al-induced root growth inhibition could be attributed to changes in cell wall polysaccharides. Although previous studies have reported that both OsSTAR1 and AtSTAR1 are involved in Al resistance, the underlying mechanism by which these STAR1 proteins affect Al resistance remains unknown (Huang et al. 2009, 2010). Here, we found that defective of AtSTAR1

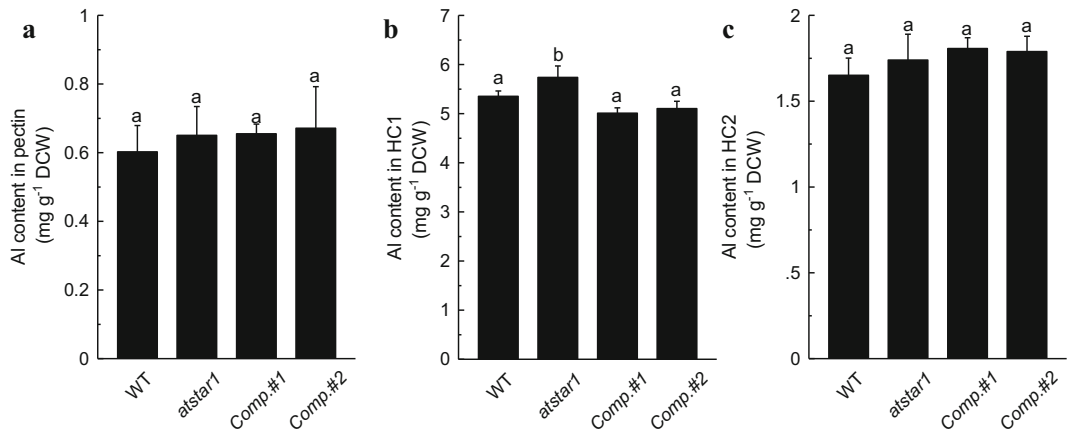

Fig. 7 Al content in pectin (a), HC1 (b) and HC2 (c) cell wall matrix polysaccharides. The different compositions of cell wall were extracted from root of 4-week-old WT, atstar1 and FeSTAR1 complemented transgenic lines under 50 μM Al treatment for 24 h. Al content was determined by ICP-OES. Data are means ± SD (n = 3). Different letters indicate significant differences at $p < 0.05$ by Tukey'st test

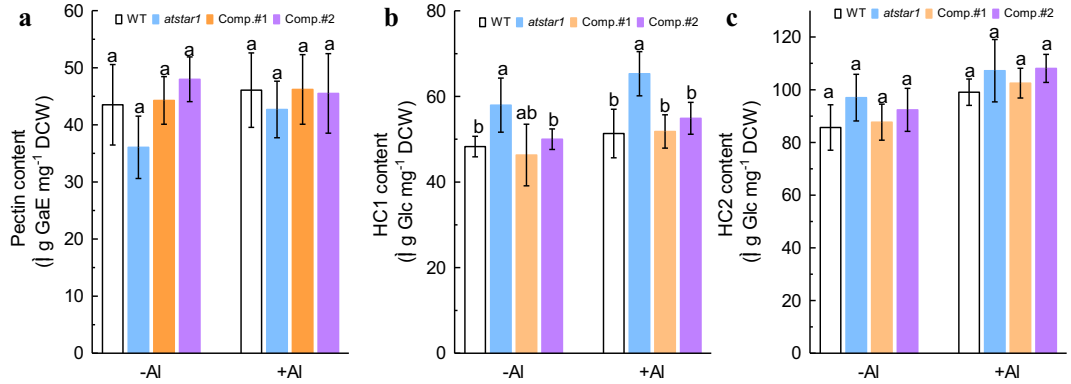

Fig. 8 Content of pectin (a), HC1 (b) and HC2 (c). The different compositions of cell wall were extracted from root of 4-week-old WT, *atstar1* and FeSTAR1 complemented transgenic lines under 50 μM Al treatment for 24 h. Data are means ± SD ($n = 3$). Different letters indicate significant differences at $p < 0.05$ by Tukey'st test

in *atstar1* mutants resulted in significant increase of cell wall Al in comparison with WT plants, whilst two FeSTAR1 complemented lines recovered Al accumulation in cell wall (Fig. 6). More specifically, when different cell wall matrix polysaccharides were analyzed, STAR1 protein consistently changed only Al accumulation in HC1 fraction, which was coincident with STAR1-mediated changes of HC1 content (Figs. 7 & 8). Therefore, it seems that STAR1 protein regulates Al resistance by specifically affecting HC1 metabolism, which contributes to Al accumulation. Consistent with this present result, it has been previously reported that cell wall HC1 contributes more significantly to Al accumulation than pectin and HC2 in Arabidopsis roots (Yang et al. 2011). What's more, in a xyloglucan reducing mutant, *xth31*, the binding of Al to cell wall was found to be greatly reduced, which as a consequence increased Al resistance (Zhu et al. 2012).

In rice, OsSTAR1 interacts with OsSTAR2 to form a bacterial-type ABC transporter, which is able to transport UDP-Glucose to apoplast in which UDP-Glucose modifies cell walls thereby preventing Al binding to cell walls (Huang et al. 2009). In contrast, Dong et al. (2017) reported that the complex protein of AtSTAR1 and AtALS3 failed to deliver UDP-Glucose when expressed in oocyte. In the present study, we found that exogenous applied UDP-Glucose could alleviate Al-induced root growth inhibition in atstar1 mutant (Fig. 5). We could infer that buckwheat FeSTAR1 regulates Al resistance by virtue of a similar mechanism with rice OsSTAR1, although question remains open whether FeSTAR1 could interact with STAR2/ALS3 proteins. At present, we have not much evidence to support the role of UDP-Glucose in cell wall modification. Nonetheless, there is some circumstantial evidence. First, UDP-Glucose is the activated form of glucose, which can be the sugar donor to biosynthesize the matrix polysaccharides catalyzed by UDP glycosyltransferases (UGTs) (Ross et al. 2001). This possibility is supported by the finding that UGTs could catalyze the glucose conjugation of monolignols, which is essential for normal cell wall lignification (Lin et al. 2016). Second, conserved domain analysis suggests that STAR1 proteins belong to PstB phosphate transporter subfamily of ABC superfamily. Therefore, it is possible that FeSTAR1 could transport phosphate in the form of UDP-Glucose. Finally, FeSTAR1 has NBD domain which contains the conserved ABC sequence motifs involved in ATP binding. Although further investigations are required, the conserved NBD domain is possibly able to bind UDP too.

We could make two possible extrapolations from the result that exogenous applied UDP-Glucose could alleviate Al-induced root growth inhibition in atstar1 mutant. One is that UDP-Glucose could modify cell wall polysaccharides in situ. However, exogenous applied UDP-Glucose failed to alleviate Al-induced root growth inhibition in WT plants, ruling out this possibility. The other is that UDP-Glucose needs to be delivered into cytoplasm in which it participates in cell wall polysaccharides metabolism. In fact, the matrix polysaccharides are synthesized by membrane-bound glycosyltransferases in the Golgi apparatus and are delivered to the cell wall via exocytosis of tiny vesicles. This might explain why exogenous applied UDG-Glucose had no effects on Al resistance of Arabidopsis WT plants as well as in rice

(Fig. 5; Huang et al. 2009). This might also be responsible to only partial recovery of exogenous applied UDP-Glucose for Al-induced root growth inhibition, because exogenous UDP-G could not enter into cytosol easily. The cytoplasm location of FeSTAR1 reinforces the intracellular utilization of UDP-Glucose (Fig. 3).

Despite the functional similarity, FeSTAR1 has distinct characteristics. First, the expression pattern differs among FeSTAR1, AtSTAR1 and OsSTAR1. The expression of both FeSTAR1 and OsSTAR1 was induced by Al stress but AtSTAR1 is constitutively expressed (Fig. 2; Huang et al. 2009, 2010). This may be one of possible reasons for much higher Al resistance of rice and buckwheat than Arabidopsis. In addition, the expression of buckwheat FeSTAR1 was induced by Al both in roots and shoots, which is different from that of rice and Arabidopsis (Fig. 2; Huang et al. 2009, 2010). Because buckwheat belongs to an Al accumulator species, it seems likely that the expression induction of FeSTAR1 in shoots is necessary for detoxifying cell wall Al in shoots. Second, the subcellular location is not consistent. OsSTAR1 is present at vesicle membranes (Huang et al. 2009). However, the complex protein of AtSTAR1 and AtALS3 was reported to be localized to tonoplast (Dong et al. 2017). By contrast, our ectopic expression of FeSTAR1-GFP fusion protein in Arabidopsis found that it was localized at both cytoplasm and nucleus (Fig. 3). In the future, it is urgent to investigate whether interaction of FeSTAR1 with STAR2/ALS3 proteins will change its subcellular location.

In summary, our results indicate that FeSTAR1 is involved in Al resistance via possibly cell wall matrix polysaccharides metabolism in buckwheat.

Acknowledgements This work was supported financially by the Natural Science Foundation of China (31572193) and The Chang Jiang Scholars Program (JLY). We are grateful to Prof. Chaofeng Huang for providing us the Arabidopsis mutant atstar1 seeds.

References

Blumenkrantz N, Asboe-Hansen G (1973) New method for quantitative determination of uronic acids. Anal Biochem 54:484–489

Bojórquez-Quintal E, Escalante-Magaña C, Echevarría-Machado I, Martínez-Estévez M (2017) Aluminum, a friend or foe of higher plants in acid soils. Front Plant Sci 8:1767

Chen WW, Xu JM, Jin JF, Lou HQ, Fan W, Yang JL (2017) Genome-wide transcriptome analysis reveals conserved and distinct molecular mechanisms of Al resistance in buckwheat (*Fagopyrum esculentum* Moench) leaves. Int J Mol Sci 18: 1859

Delhaize E, Ryan PR (1995) Aluminum toxicity and tolerance in plants. Plant Physiol 107:315–321

Dong J, Pineros MA, Li X, Yang H, Liu Y, Murphy AS, Kochian LV, Liu D (2017) An Arabidopsis ABC transporter mediates phosphate deficiency-induced remodeling of root architecture by modulating iron homeostasis in roots. Mol Plant 10: 244–259

Dubois M, Gille KA, Hamilton JK, Rebers PA, Smith F (1956) Colorimetric method for determination of sugars and related substances. Anal Chem 28:350–356

Huang CF, Yamaji N, Mitani N, Yano M, Nagamura Y, Ma JF (2009) A bacterial-type ABC transporter is involved in aluminum tolerance in rice. Plant Cell 21:655–667

Huang CF, Yamaji N, Ma JF (2010) Knockout of a bacterial-type ATP-binding cassette transporter gene, AtSTAR1, results in increased aluminum sensitivity in Arabidopsis. Plant Physiol 153:1669–1677

Jefferson RA, Kavanagh TA, Bevan MW (1987) GUS fusions: beta-glucuronidase as a sensitive and versatile gene fusion marker in higher plants. EMBO J 6:3901–3907

Keegstra K (2010) Plant cell walls. Plant Physiol 154:483–486

Klug B, Horst WJ (2010) Oxalate exudation into the root-tip water free space confers protection from aluminum toxicity and allows aluminum accumulation in the symplast in buckwheat (*Fagopyrum esculentum*). New Phytol 187:380–391

Kochian LV (1995) Cellular mechanisms of aluminum toxicity and resistance in plants. Annu Rev Plant Biol 46:237–245

Lei GJ, Yokosho K, Yamaji N, Fujii-Kashino M, Ma JF (2017a) Functional characterization of two half-size ABC transporter genes in aluminium-accumulating buckwheat. New Phytol 215:1080–1089

Lei GJ, Yokosho K, Yamaji N, Ma JF (2017b) Two MATE transporters with different subcellular localization are involved in Al tolerance in buckwheat. Plant Cell Physiol 58: 2179–2189

Lin J-S, Huang X-X, Li Q, Cao Y, Bao Y, Meng X-F, Li Y-J, Fu C, Hou B-K (2016) UDP-glycosyltransferase 72B1 catalyzes the glucose conjugation of monolignols and is essential for the normal cell wall lignification in *Arabidopsis thaliana*. Plant J 88:26–42

Ma JF, Hiradate S (2000) Form of aluminium for uptake and translocation in buckwheat (*Fagopyrum esculentum* Moench). Planta 211:355–360

Ma JF, Hiradate S, Matsumoto H (1998) High aluminum resistance in buckwheat. II Oxalic acid detoxifies aluminum internally Plant Physiol 117:753–759

Reyna-Llorens I, Corrales I, Poschenrieder C, Barcelo J, Cruz-Ortega R (2015) Both aluminum and ABA induce the expression of an ABC-like transporter gene (*FeALS3*) in the Al-tolerant species *Fagopyrum esculentum*. Environ Exp Bot 111:74–82

Ross J, Li Y, Lim EK, Bowles DJ (2001) Higher plant glycosyltransferases. Genome Biol 2:3004

Shen R, Ma JF, Kyo M, Iwashita T (2002) Compartmentation of aluminium in leaves of an Al-accumulator, *Fagopyrum esculentum* Moench. Planta 215:394–398

Shen R, Iwashita T, Ma JF (2004) Form of Al changes with Al concentration in leaves of buckwheat. J Exp Bot 55:131–136

Tang QY, Zhang CX (2012) Data processing system (DPS) software with experimental design, statistical analysis and data mining developed for use in entomological research. Insect Sci 20:254–260

Von Uexküll HR, Mutert E (1995) Global extent, development and economic impact of acid soils. Plant Soil 171:1–15

Xu JM, Fan W, Jin JF, Lou HQ, Chen WW, Yang JL, Zheng SJ (2017) Transcriptome analysis of Al-induced genes in buckwheat (*Fagopyrum esculentum* Moench) root apex: new insight into Al toxicity and resistance mechanisms in an Al accumulating species. Front Plant Sci 8:1141

Yang JL, Zheng SJ, He YF, Tang C, Zhou G (2005) Genotypic differences among plant species in response to aluminum stress. J Plant Nutr 28:949–961

Yang JL, Li YY, Zhang YJ, Zhang SS, Wu YR, Wu P, Zheng SJ (2008) Cell wall polysaccharides are specifically involved in the exclusion of aluminum from the rice root apex. Plant Physiol 146:602–611

Yang JL, Zhu XF, Peng YX, Zheng C, Li GX, Liu Y, Shi YZ, Zheng SJ (2011) Cell wall hemicellulose contributes significantly to aluminum adsorption and root growth in Arabidopsis. Plant Physiol 155:1885–1892

Yokosho K, Yamaji N, Ma JF (2014) Global transcriptome analysis of Al-induced genes in an Al-accumulating species, common buckwheat (*Fagopyrum esculentum* Moench). Plant Cell Physiol 55:2077–2091

Zhang L, Li X, Ma B, Gao Q, du H, Han Y, Li Y, Cao Y, Qi M, Zhu Y, Lu H, Ma M, Liu L, Zhou J, Nan C, Qin Y, Wang J, Cui L, Liu H, Liang C, Qiao Z (2017) The tartary buckwheat genome provides insights into rutin biosynthesis and abiotic stress tolerance. Mol Plant 10:1224–1237

Zheng SJ, Ma JF, Matsumoto H (1998) High aluminum resistance in buckwheat: I. Al-induced specific secretion of oxalic acid from root tips. Plant Physiol 117:745–751

Zheng SJ, Yang JL, He YF, Yu XH, Zhang L, You JF, Shen RF, Matsumoto H (2005) Immobilization of aluminum with phosphorus in roots is associated with high aluminum resistance in buckwheat. Plant Physiol 138:297–303

Zhu XF, Shi YZ, Lei GJ, Fry SC, Zhang BC, Zhou YH, Braam J, Jiang T, Xu XY, Mao CZ (2012) XTH31, encoding an in vitro XEH/XET-active enzyme, regulates aluminum sensitivity by modulating in vivo XET action, cell wall xyloglucan content, and aluminum binding capacity in Arabidopsis. Plant Cell 24:4731–4747

Zhu H, Wang H, Zhu Y, Zou J, Zhao FJ, Huang CF (2015) Genome-wide transcriptomic and phylogenetic analyses reveal distinct aluminum-tolerance mechanisms in the aluminum accumulating species buckwheat (*Fagopyrum tataricum*). BMC Plant Biol 15:16